INSTITUTE OF TECHNOLOGY

AIR UNIVERSITY

UNITED STATES AIR FORCE

SCHOOL OF ENGINEERING

THESIS

WRIGHT-PATTERSON AIR FORCE BASE, OHIO

AF-WP-B-SEP 60 5M

A FEASIBILITY STUDY OF A

MAGNETO-HYDRODYNAMIC CENTRIFUGE

THESIS

Presented to the Faculty of the School of Engineering

The Institute of Technology

Air University

in Partial Fulfillment of the

Requirements for the

Master of Science Degree

in Electrical Engineering

By

Luin Blunt Ricks, B.S.

Captain, USAF

GE-61

August 1961

PREFACE

This report is the result of my attempt to present the findings of a feasibility study of a magneto-hydrodynamic centrifuge. I have found this study both interesting and rewarding - especially since I can answer in the affirmative to the basic question of "Will it work?" Since feasibility research is preliminary in nature, I have included qualitative observations and recommendations whenever they seemed to be pertinent to future investigation.

I gratefully acknowledge the effort and patience required of Mr. M. Wolfe and the personnel of the Institute Workshop who helped build the "thing." Also, I would like to thank Mr. M. W. Corbin and the personnel of the Electrical Engineering laboratories for their understanding and tolerance after I had melted four power cables and horribly abused a power rectifier.

Finally, it is with a sincere sense of indebtedness that I thank Major E. T. Garrett of the Electrical Engineering Department who originally proposed the idea of a magneto-hydrodynamic centrifuge and the basic configuration of the development prototype. Major Garrett was a constant source of encouragement and help throughout the project.

Contents

List of Figures

List of Symbols

A	annulus area
$\vec{B}$	magnetic flux density vector
$\vec{D}$	electric displacement vector
$\vec{E}$	electric field vector
F	total force
$\vec{f}$	force vector per unit volume
$\vec{H}$	magnetic field vector
I	current
$\vec{j}$	current density vector
ℓ	annulus length
M	Hartmann Number
P	pressure
$\vec{q}$	mercury velocity vector
Re	Reynold's Number
V_a	armature or annulus voltage
V_i	induced voltage
δ	annulus width
ε	permittivity
μ	absolute viscosity
$\bar{\mu}$	permeability
ν	kinematic viscosity
ρ	mass density
σ	electric conductivity
θ_0	electric body force per unit volume

ABSTRACT

The magneto-hydrodynamic centrifuge is a direct-current motor with a mercury armature. Centrifuging action is derived from the rotating mercury which, at sufficient speeds, assumes the shape of a hollow ring. A development prototype is designed and tested in order to determine the feasibility of such a centrifuge. Test results were promising and indicated that the basic operational principle is sound and feasible. A paddle wheel was rotated at 2000 RPM by a rotating ring of mercury at an estimated mercury input power of 5 watts.

A FEASIBILITY STUDY OF A

MAGNETO-HYDRODYNAMIC CENTRIFUGE

I. Introduction

The term "magneto-hydrodynamics" has, in recent years, been used to denote the theory of the flow of an electrically conducting fluid in the presence of a magnetic field. The force equation of electromagnetic theory shows that a current-carrying conductor will experience a force if it is properly orientated in a magnetic field. Similarly, if a fluid which is a conductor of electricity is subjected to a magnetic field, an electric body force is produced. A body force in fluid dynamics is any force that is applied directly to the fluid elements. This reaction is distinguished from pressure, for example, which is a force between adjacent particles. The Faraday or electromagnetic pump is basically a magneto-hydrodynamic device which uses electric body force to pump liquid metals such as mercury.

This paper is concerned with the study of a magneto-hydrodynamic centrifuge which uses electric body force to drive mercury around an annulus formed by the pole faces of an electro-magnet. This centrifuge is essentially a direct-current motor with a mercury armature. At high rotational speeds, the mercury assumes the shape of a ring in the annulus. The remaining space of the annulus forms a chamber in which materials of different densities might be separated by the centrifugal forces derived from the rotating mercury.

The purpose of this report is to present the findings of a feasibility study of a development prototype. In order to accomplish this purpose, the following aspects of the problem are included in the report: (1) an outline of the underlying theory of the centrifuge; (2) a description of the prototype model used; (3) performance data; (4) conclusions from a feasibility viewpoint; and (5) a discussion of difficulties encountered and recommendations for further development. This study was initiated mainly because of the advantage of having a centrifuge with only one moving part - the mercury armature. As such, the magneto-hydrodynamic centrifuge has theoretically high centrifugal forces at low power inputs. Also, a possibility exists that the centrifuge could be used as a positive flow device in which materials could be separated continuously.

Experiments were confined to one configuration; however, the experimental prototype used seems to be basic for a direct-current motor principle. Primary consideration is given to the velocity and stability characteristics of the preliminary design, and no attempt to centrifuge materials was made.

II. Theory

General

If a fluid is a conductor of electricity, then the laws of electromagnetic theory must be dealt with in addition to the laws of fluid dynamics whenever the magnitude of magnetic and electric fields require consideration. There is an additional reaction called "electric body force" which is the counterpart of the force that drives an electric motor. The fundamental equation for the force exerted on a wire of length ℓ carrying a current in a magnetic field $\vec{B}$ is

$$\vec{F} = \vec{i}\,\ell \times \vec{B} \tag{1}$$

Equation (1) shows that force is given by the vector product of the current and magnetic field and is therefore perpendicular to both. In the case of a fluid, we are concerned with current passage through a volume rather than a wire. If the current density vector $\vec{j}$ in amperes per unit area is used, then the body force per unit volume is given by the vector equation

$$\vec{\xi} = \vec{j} \times \vec{B} \tag{2}$$

A fluid carrying electricity experiences another basic phenomenon which is Joule heating. The familiar formula I^2R becomes, in this application

$$\text{Heat released per unit volume per unit time} = j^2/\sigma \tag{3}$$

where σ denotes conductivity. Considering the high conductivity of mercury, Joule heating is usually neglected in its application to fluid dynamic equations involving the flow of mercury.

A completely general fluid momentum equation which includes electric body force can be written as

$$\rho\, d\vec{q}/d\tau + \nabla P = \vec{j} \times \vec{B} + \mu\left[\nabla^2\vec{q} + \frac{1}{3}\nabla\nabla\cdot\vec{q}\right] \tag{4}$$

where ρ, q, P, μ are the mass density, velocity, pressure, and viscosity of the fluid (Ref. 1:236). If mercury is assumed to be incompressible, then equation (4) becomes

$$\rho\, d\vec{q}/d\tau + \nabla P = \vec{j} \times \vec{B} + \mu\nabla^2\vec{q} \tag{5}$$

Notice that the term $\vec{j} \times \vec{B}$ or $\vec{f}$ shows up in the equation as a forcing function for the acceleration term $\rho\, d\vec{q}/d\tau$ on the left. Relationship (5) is known as the Navier-Stokes Equation for incompressible flow. The term $\frac{1}{3}\nabla\nabla\cdot\vec{q}$ is zero because the continuity equation shows that for incompressible flow

$$\nabla \cdot \vec{q} = 0 \tag{6}$$

Since electric and magnetic fields are present in the fluid, Maxwell's equations must be accounted for in order to be completely general. If time varying components of fields are zero, then Maxwell's equations become

$$\nabla \times \vec{H} = \vec{j} \tag{7}$$

$$\vec{D} = \varepsilon \vec{E} \tag{8}$$

$$\nabla \times \vec{E} = 0 \tag{9}$$

$$\vec{B} = \bar{\mu} \vec{H} \tag{10}$$

$$\nabla \cdot \vec{D} = \rho_{\varepsilon} \tag{11}$$

where $\vec{H}$ is the magnetic field vector; $\vec{j}$, current vector; $\vec{D}$, electric displacement vector; ε , permittivity of mercury; $\vec{E}$, electric field vector; $\vec{B}$, magnetic induction vector; $\bar{\mu}$, permeability of mercury; and ρ_{ε} , charge density. The charge density or divergence of the electric displacement vector is, in this case, essentially zero in view of the high conductivity of mercury. From the simplified Maxwell's equations the Generalized Ohm's Law becomes

$$\vec{j} = \sigma \left[\vec{E} + \bar{\mu} (\vec{g} \times \vec{H}) \right] \tag{12}$$

Equation (12) has a direct analogy to the familiar direct-current motor formula

$$V_a = I R + V_i \tag{13}$$

where V_a , I , and R are the applied voltage, current, and resistance of the armature; and V_i is the back electromotive force. If (13) is solved for I , then

$$I = \frac{1}{R} (V_a - V_i) \tag{14}$$

Comparing equation (14) to (12), it is seen that the induced voltage in a fluid carrying electricity is

$$V_i = \bar{\mu}\,(\vec{q} \times \vec{H}) \tag{15}$$

Equation (15) is a general statement of the generator principle relationship which states that

$$V_i = l\,\vec{B} \times \vec{q} \tag{16}$$

where V_i is the induced voltage on a conductor of length l moving at a velocity q in a magnetic field. Equation (15) states the same condition except that V_i is expressed per unit length.

Again comparing (14) to (12), it is seen that the ohmic drop across a conducting fluid per unit length is

$$\text{ohmic drop/unit length} = \vec{j}/\sigma \tag{17}$$

The general theory discussed above will now be applied to the specific problem of mercury rotating in an annulus under the influence of steady electro-magnetic fields.

<u>Theory Applied to Mercury Rotating in An Annulus</u>

The general Navier-Stokes equation for incompressible flow can be written in cylindrical coordinates as follows:

$$\rho\left[dq_r/dt - q_\theta^2/r\right] = R_0 - \partial P/\partial r + \mu\left[\nabla^2 q_r - q_r/r^2 - \frac{2}{r^2}\,\partial q_\theta/\partial\theta\right] \tag{18}$$

$$\rho\left[dq_\theta/dt + q_r q_\theta/r\right] = \Theta_0 - \frac{1}{r}\,\partial P/\partial\theta + \mu\left[\nabla^2 q_\theta + \frac{2}{r^2}\,\partial q_r/\partial\theta - q_\theta/r^2\right] \tag{19}$$

$$\rho \, dq_z/d\tau = Z_0 - \partial p/\partial z + \mu \nabla^2 q_z \qquad (20)$$

Where R_0 , θ_0 , and Z_0 are electric body forces per unit volume and the operator ∇^2 is

$$\nabla^2 = \frac{\partial^2}{\partial r^2} + \frac{1}{r}\frac{\partial}{\partial r} + \frac{1}{r^2}\frac{\partial^2}{\partial \theta^2} + \frac{\partial^2}{\partial z^2} \qquad (21)$$

Next, consider the rotating section of mercury in Fig. 1 on this page with orientation of the variables as shown.

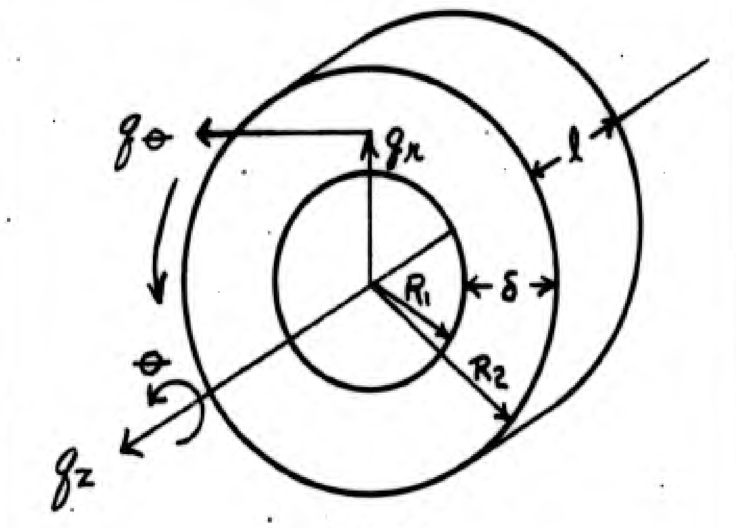

Fig. 1

Rotating Section of Mercury

The following assumptions are now made:

1. The magnetic flux in the annulus has only an r component which is uniform and constant as a function of θ and z .
2. The current density vector $\vec{j}$ has only a z component which is uniform and constant throughout the volume of mercury.

3. Only steady motion is present.

4. q_θ is the only velocity component present.

From the first two assumptions, magnetic flux and current are mutually perpendicular; the only body force present, therefore, is θ_o. The third assumption requires a zero value for all time derivatives. The assumption that q_r and q_z is zero essentially requires flow to be laminar without three dimensional mixing such as that caused by turbulence. Considering the above assumptions, the reduced Navier-Stokes equations now become

$$\rho \, q_\theta^2 / r = dP/dr \tag{22}$$

$$0 = \Theta_0 + \mu \left[\partial^2 q_\theta / \partial r^2 + \frac{1}{r} \partial q_\theta / \partial r - q_\theta / r^2 + \partial^2 q_\theta / \partial z^2 \right] \tag{23}$$

The significance of equation (22) can be found from Fig. 2 of this page.

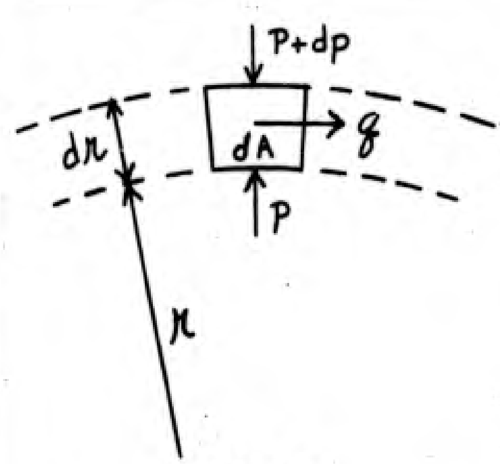

Fig. 2

Flow in a Curved Path

(From Ref. 2:138)

Imagine the flow of a particle between two concentric stream lines as shown. The radius of curvature is r , and q_θ is the tangential linear velocity of the infinitesimal element of height dr and area dA . The mass of this element is given by

$$m = \rho \, dr \, dA \tag{24}$$

where ρ is the mass density. Centrifugal force is then

$$C.F. = m q_\theta^2 / r = \rho \, dr \, dA \, q_\theta^2 / r \tag{25}$$

The pressure varies from p to $p + dp$ as the radius increases from r to $r + dr$. Since the force on the outer surface counteracts the centrifugal force, an expression for $dp\,dA$ becomes

$$dp\,dA = \rho \, dr \, dA \, q_\theta^2 / r \tag{26}$$

Solving (26) for $\rho q_\theta^2 / r$ yields the same results as given in equation (22), which was reduced from Navier-Stokes equation. The importance of equation (22) will be brought out further during the discussion of mercury velocity measurements.

If the thickness of a ring of mercury rotating in an annulus is small compared to the annulus depth, the reduced Navier-Stokes equation (23) becomes

$$0 = \theta_0 + \mu \left(d^2 q_\theta / dr^2 + \frac{1}{r} \, dq_\theta / dr - q_\theta^2 / r \right) \tag{27}$$

Solving equation (27) for q_θ (see Appendix, page 46) yields

$$q_\theta(r) = A_1 r^{-1} + A_2 r - \frac{\theta_0}{3\mu} r^2 \tag{28}$$

The constants A1 and A2 can be evaluated by applying appropriate boundary conditions dictated by boundary layer theory. In fluid dynamics, boundary layer theory states that fluid velocity is zero next to the wall or boundary containing a fluid. In the present case of a fluid flowing between concentric cylinders, the boundary conditions are

$$g_\theta(R_1) = 0 = A_1 R_1^{-1} + A_2 R_1 - \frac{\theta_0}{3\mu} R_1^2 \tag{29}$$

$$g_\theta(R_2) = 0 = A_1 R_2^{-1} + A_2 R_2 - \frac{\theta_0}{3\mu} R_2^2 \tag{30}$$

If equations (29) and (30) are solved simultaneously for the constants A_1 and A_2, $g_\theta(r)$ becomes

$$g_\theta(r) = \frac{\theta_0}{3\mu}\left[\left(\frac{R_2^3 - R_1^3}{R_2^2 - R_1^2}\right) r - \left(\frac{R_1^2 R_2^2}{R_1 + R_2}\right)\frac{1}{r} - r^2\right] \tag{31}$$

where $R_1 < r < R_2$

The expression for electric body force per unit volume was given previously as

$$\vec{f} = \vec{j} \times \vec{B} \tag{2}$$

Since in our present case only θ_0 is considered, (2) becomes

$$\theta_0 = \vec{j_z} \times \vec{B_r} \,. \tag{32}$$

The area through which $\vec{j_z}$ passes in an annulus is

$$\pi(R_2^2 - R_1^2) \tag{33}$$

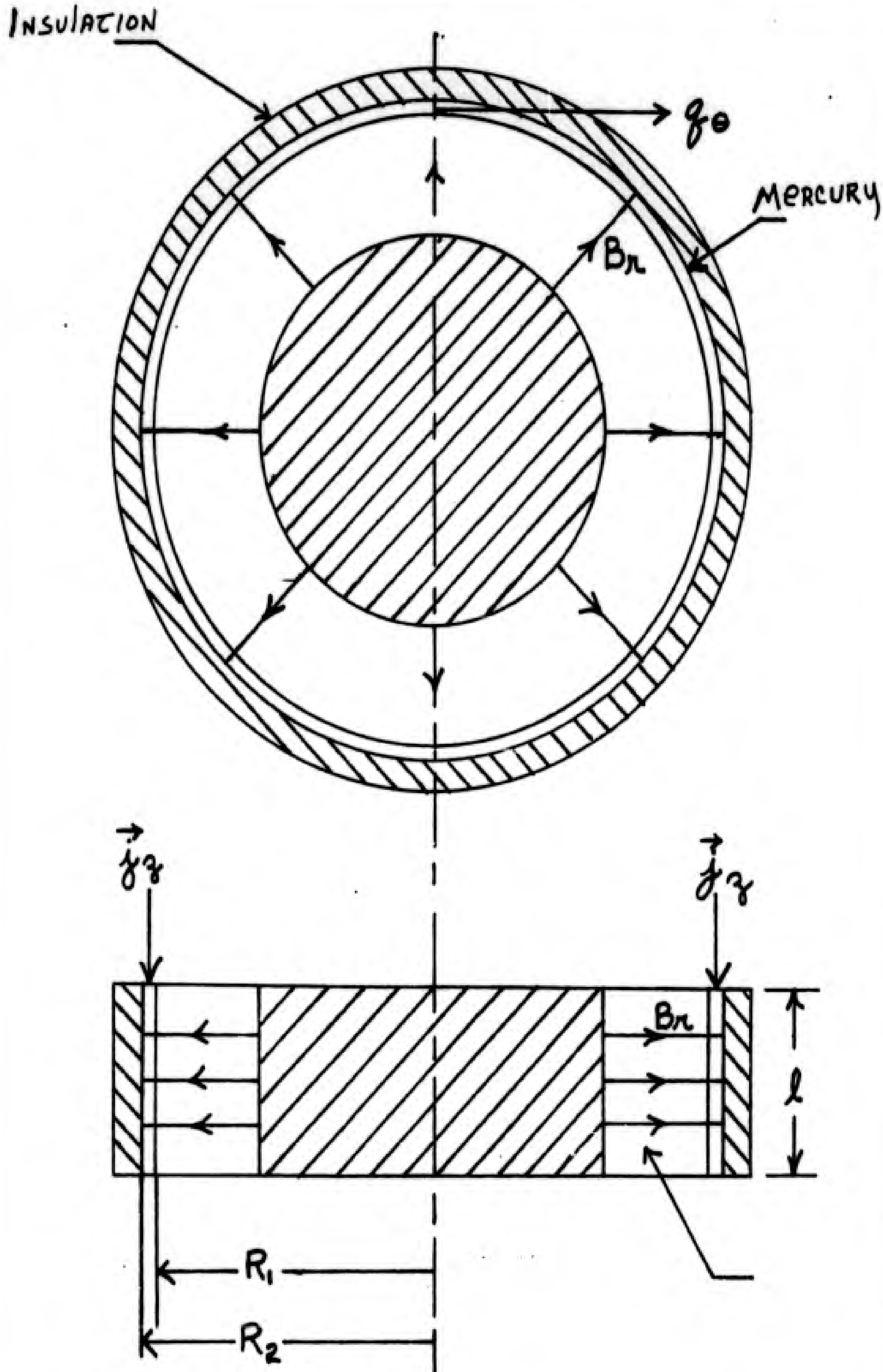

Illustration of Physical
and Electro-Magnetic Quantities

Fig. 3

If the total current is expressed in abamperes, the magnetic flux density in gauss per square centimeter, and R in centimeters, then θ_0 in dynes per cubic centimeter is

$$\theta_0 = IB \Big/ \pi(R_2^2 - R_1^2) \tag{34}$$

Vector notation is dropped in (34) because $\vec{j}$ and $\vec{B}$ were assumed to be mutually perpendicular.

The remaining physical quantity is back electromotive force per unit length, which from equation (15) is

$$V_i = g_\theta B r \tag{35}$$

Here it is assumed that mercury permeability is equal to that of free air.

As a final analysis, suppose that an annulus is only partly filled with mercury which is rotating fast enough to form a hollow ring. Figure 3 facing this page illustrates the configuration and pertinent physical and electromagnetic quantities. The general solution to the Navier-Stokes equation still applies and it is repeated here.

$$g_\theta(r) = A_1 r^{-1} + A_2 r - \frac{\theta_0}{3\mu} r^2 \tag{27}$$

The only difference between the evaluation of equation (27) for a full annulus and for a rotating ring lies in the choice of boundary conditions. The inner surface of the rotating ring has a velocity

V_0 , and again the velocity is zero at the containing wall. Imposing these conditions on equation (27) yields

$$q_\theta(R_1) = V_0 = A_1 R_1^{-1} + A_2 R_2 - \frac{\theta_0}{3\mu} R_1^2 \tag{36}$$

$$q_\theta(R_2) = 0 = A_1 R_2^{-1} + A_2 R_2 - \frac{\theta_0}{3\mu} R_2^2 \tag{37}$$

After solving (36) and (37) for A1 and A2, the expression for q_θ becomes

$$q_\theta(r) = \left[\frac{R_1 R_2}{(R_2^2-R_1^2)} V_0 - \frac{\theta_0}{3\mu} \frac{R_1^2 R_2^2}{(R_1+R_2)}\right] \frac{1}{r}$$

$$+ \left[\frac{\theta_0}{3\mu}\left(\frac{R_2^3-R_1^3}{R_2^2-R_1^2}\right) - \frac{R_1 V_0}{(R_2^2-R_1^2)}\right] r - \frac{\theta_0}{3\mu} r^2 \tag{38}$$

Equation (38) is indeterminate unless some empirical relationship between V_0 and θ_0 is found from experimental data. Although (38) is similar to the solution of Navier-Stokes equations for flow between an inner rotating cylinder and a stationary outer cylinder, there is a basic difference. In the latter case a known velocity of an inner rotating cylinder imparts torque to the fluid. Equation (38) shows that a body force and an unknown velocity determines the velocity profile.

The expressions for V_i and θ_0 in the case of a rotating ring remain the same as equations (34) and (35) respectively which were found in the case of a full annulus.

Knowing the dimensions of an annulus, equation (34) may be solved for θ_0 if values of current and magnetic flux are known. Since the thickness of the annulus ring is given by

$$\delta = R_2 - R_1 \tag{39}$$

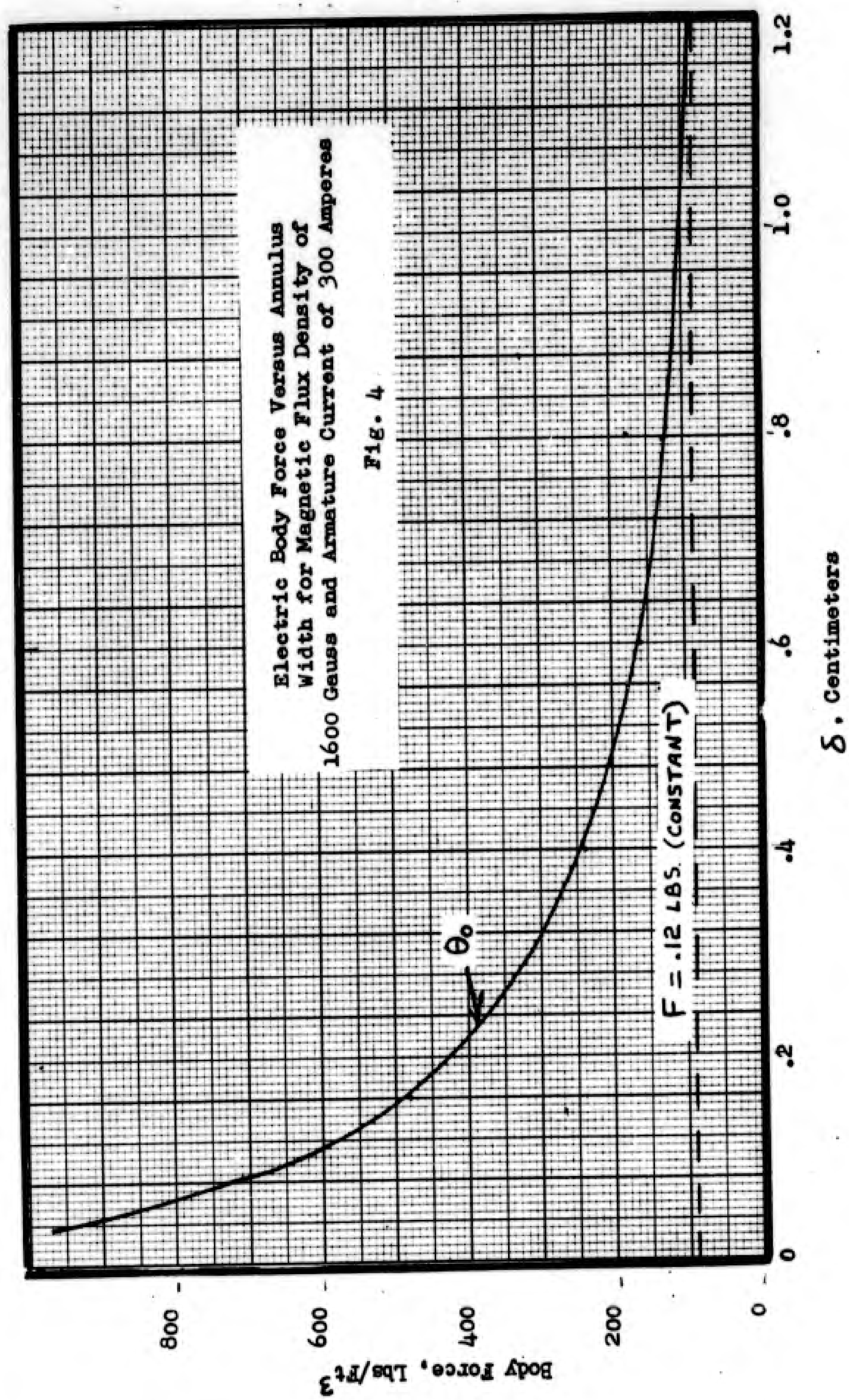

Electric Body Force Versus Annulus Width for Magnetic Flux Density of 1600 Gauss and Armature Current of 300 Amperes

Fig. 4

A plot may be constructed showing electric body force as a function of δ. Figure 4 on page 13 shows a graph of θ_0 versus δ using the dimensions of the development prototype and representative experimental values of current and flux. For comparison, the total force given by

$$F = \theta_0 \times \text{Volume of Annulus} \tag{40}$$

is plotted as a function of δ. It is seen from Fig. 4 that force is small compared to θ_0 and remains constant as δ is varied, whereas θ_0 increases rapidly as δ becomes small. This increase is due to the heavy current density which occurs in a small, cross-sectional area.

It can be shown that the rotating ring of mercury is analogous to the armature of a direct-current motor. Consider Fig. 5 of this page in which the ring has a segment of mercury of mean arc ΔC and length ℓ.

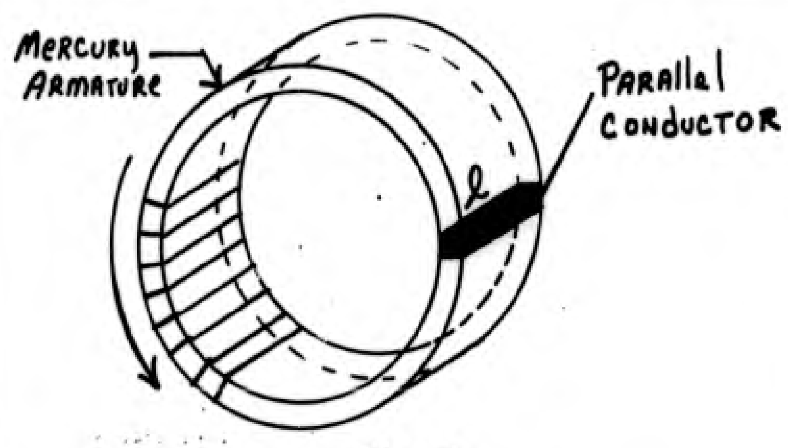

Fig. 5

Direct Current Motor Analogy

These segments are essentially parallel conductors of length which, assuming uniform current density, carry equal currents. From equation (1), the force on each segment is

$$f_s = \left[I\ell \Big/ \frac{\pi(R_1+R_2)}{\Delta C} \right] B \qquad (41)$$

where I is the total current in the annulus and $\pi(R_1+R_2)/\Delta C$ is the number of segments N. If equation (41) is multiplied by N, the total force exerted on the mercury is simply

$$F = BI\ell \qquad (42)$$

Force calculated from equation (42) is, of course, the same as force found by multiplying θ_0 by the volume of the mercury contained in the annulus. A plot of total force versus the current through the mercury is shown in Fig. 6.

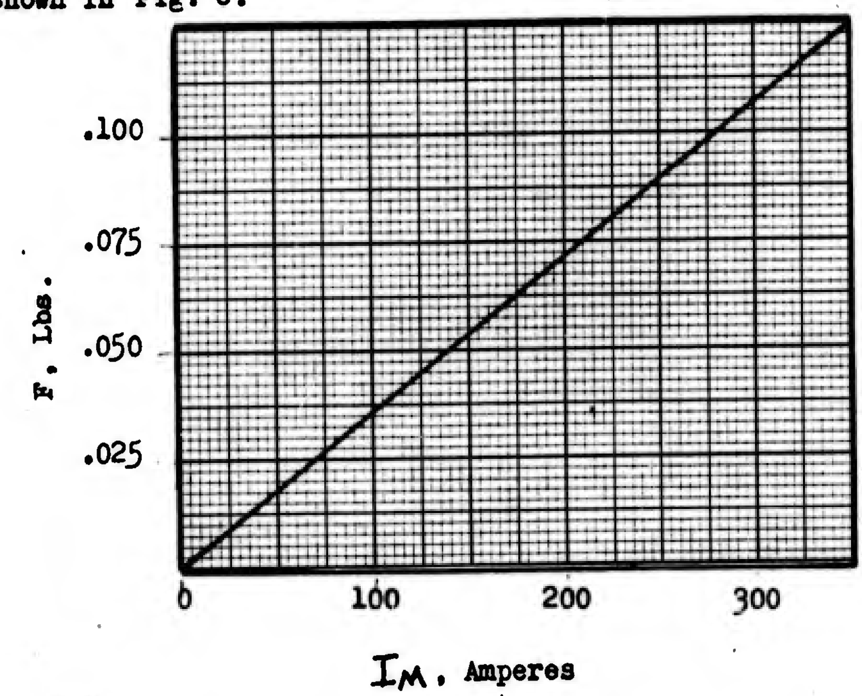

Fig. 6

Total Force Versus Armature Current for Magnetic Flux Density of 1600 Gauss

It was believed at first that the induced voltage or back electromotive force would reduce the high current requirements at higher velocities. This was not the case, however, since g_θ (average) would have to be approximately 200 ft/sec in order to produce .1 volts of back electromotive force. V_i is calculated from equation (16) by assuming average values of mercury velocity, and the results are presented in Fig. 7 of this page. Shunt, series, or compounded field windings should not produce markedly different speed characteristics as with normal direct-current rotary machines, since the induced voltage is comparable with or even smaller than ohmic drops (Ref. 3:4.9).

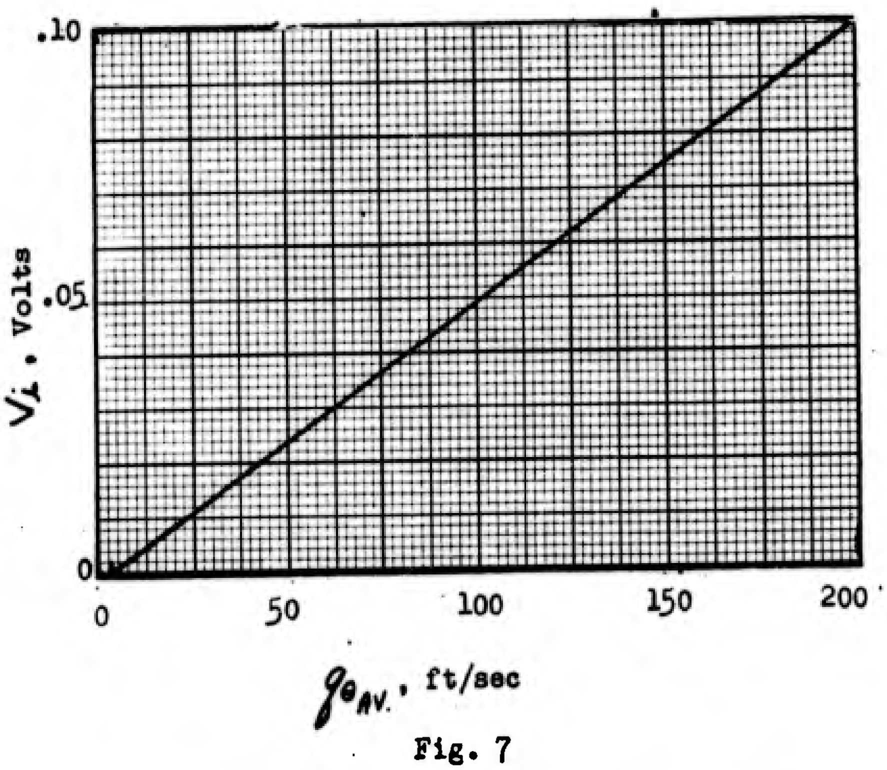

Fig. 7

Induced Voltage Versus Assumed Values of Average Mercury Velocity for Magnetic Flux Density of 1600 Gauss.

Since high values of current are involved, the effect of Joule heating in the mercury should be considered. The $I_M^2 R_M$ losses for two different values of δ were calculated and the results shown in Fig. 8.

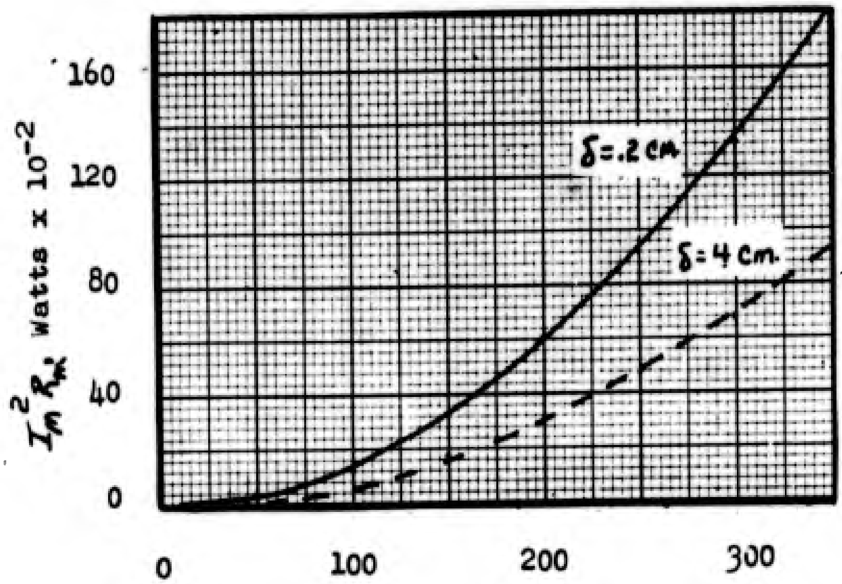

Fig. 8
Joule Heating Versus Armature Current

For the range of armature currents shown, Joule heating is not large enough to create any temperature problems.

In an attempt to predict mercury velocity, the dimensions of the annulus used in the development prototype were substituted into equation (31) which is the solution for a full annulus. If q_θ is expressed in cm/sec, and r in cm, $q_\theta(r)$ becomes

$$q_\theta(r) = \frac{\theta_0}{3\mu}\left(6.94\,r - 47.0/r - r^2\right) \qquad (43)$$

Equation (43) is based upon the assumption that δ is much smaller than ℓ which is valid for a thin ring of mercury, but not for a full annulus of the dimensions used. In effect this assumption neglects the wall shearing caused by the top and bottom surfaces of the annulus. Since these surfaces are approximately equal to the total inner and outer vertical surfaces, θ_0 is estimated to be reduced effectively by a factor of 1/2. Even with this approximation, equation (43) is valid only in the θ, r plane midway between the top and bottom of the annulus, because of the boundary layers created by the horizontal surfaces.

A further approximation had to be made because of the current distribution in the mercury when the annulus is full. Figure 9 of this page shows the actual configuration used which resulted in non-vertical currents for starting the centrifuge.

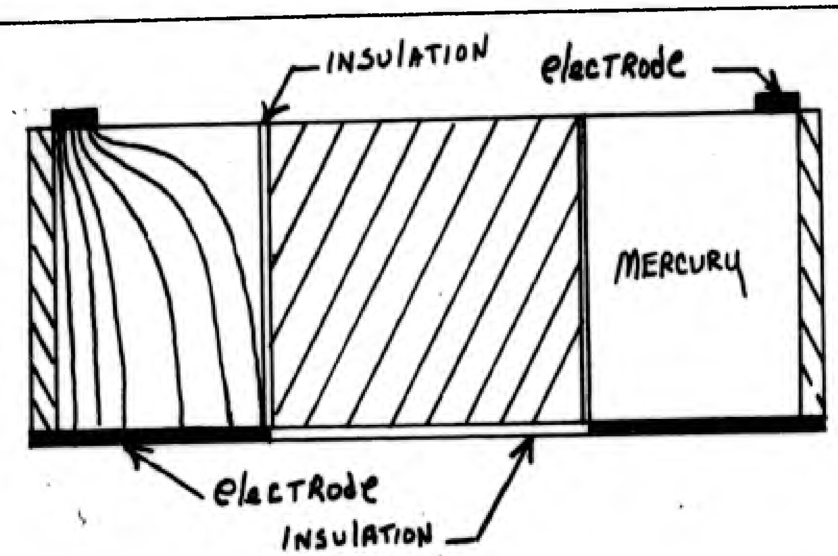

Fig. 9

Current Distribution For a
Full Annulus of Mercury

The effective angle between current and magnetic flux was estimated to be approximately 30°. Since θ_0 is given by the vector product of current density and magnetic flux density, the approximation would reduce θ_0 by another factor of 1/2.

Applying the above approximations to equation (43), $q_{\theta AV}$ was found to be 83.3 ft/sec. The usual value of Reynold's Number accepted as the dividing point between laminar and turbulent flow is given as 2300. Reynold's Number is given by the equation

$$Re = \rho V L / \mu \qquad (44)$$

where ρ , V , L , and μ are the mass density, average velocity, characteristic length, and viscosity, respectively. If equation (44) is solved using δ as a characteristic length, Re is found to be 26.8 x 10^5 at 83.3 ft/sec which far exceeds the critical Reynold's Number of 2300. R. V. Monopoli, in a paper entitled "The Development of a Magneto-hydrodynamic Gyroscope," indicated that mercury being driven in an annulus by a rotating magnetic field became turbulent at the critical Reynold's Number, 2300 (Ref. 4:372). Experimental studies have shown, however, that in the case of a steady, externally applied magnetic field, turbulence can be suppressed at unusually high Reynold's Numbers. J. Hartmann and F. Lazarus have investigated the effect of a magnetic field for the case of mercury flowing in a rectangular channel. It is shown that, if in the absence of a field the flow is turbulent, as the magnetic field is increased, turbulence is gradually suppressed and the coefficient of friction gradually increases (Ref. 5:7). Based on the work of W. Murgatroyd (Ref. 6:1348), a recent paper gives a criterion for determining the transition from laminar to turbulent flow in rectangular magneto-fluid channels (Ref. 7:798). It is shown that the transition occurs whenever

$$Re/M \cong 236 \tag{45}$$

Here Re is the Reynold's Number and M , the Hartmann Number, which is given by

$$M = BL(\sigma/\mu)^{\frac{1}{2}} \tag{46}$$

where L is again the characteristic length and σ is the conductivity of the fluid.

If the ratio of equation (45) is formed for our present case, the value of Re/M is 53.4×10^3 at $g_{\theta\,AV}$ = 83.3 ft/sec, and B = 1600 gauss. Although no empirical relationships of magnetic suppression in an annulus were found in the literature, Re/M indicates that flow is probably turbulent. If flow is turbulent, solution (27) which was found from the reduced Navier-Stokes equation is invalid because turbulence is characterized by three dimensional mixing of fluid particles. The magnetic field in the annulus is apparently not strong enough to suppress turbulence at the calculated velocity.

Equation (35) should still give reasonable approximations of velocity if the Reynold's Number is less than 2300. In addition, velocity profiles calculated from equation (35) would have the correct shape as long as flow is laminar. For $\theta_\bullet/3\mu$ equal to unity, (35) is

$$g_\theta(r) = 6.94r - 47.0/r - r^2 \tag{47}$$

Figure 10 on page 22 shows q_θ plotted as a function of r. As mentioned previously, this is the velocity profile in the θ, r plane midway between the top and bottom of the annulus.

Sample calculations of R_e, M, and turbulent transition estimates are included in the Appendix. The case of turbulent flow defies a rigorous mathematical solution even if magnetic effects are ignored (Ref. 7:796). Experimental data seem to be more suitable for determining the velocity characteristics of a mercury ring, and these data are presented after a description of the experimental apparatus.

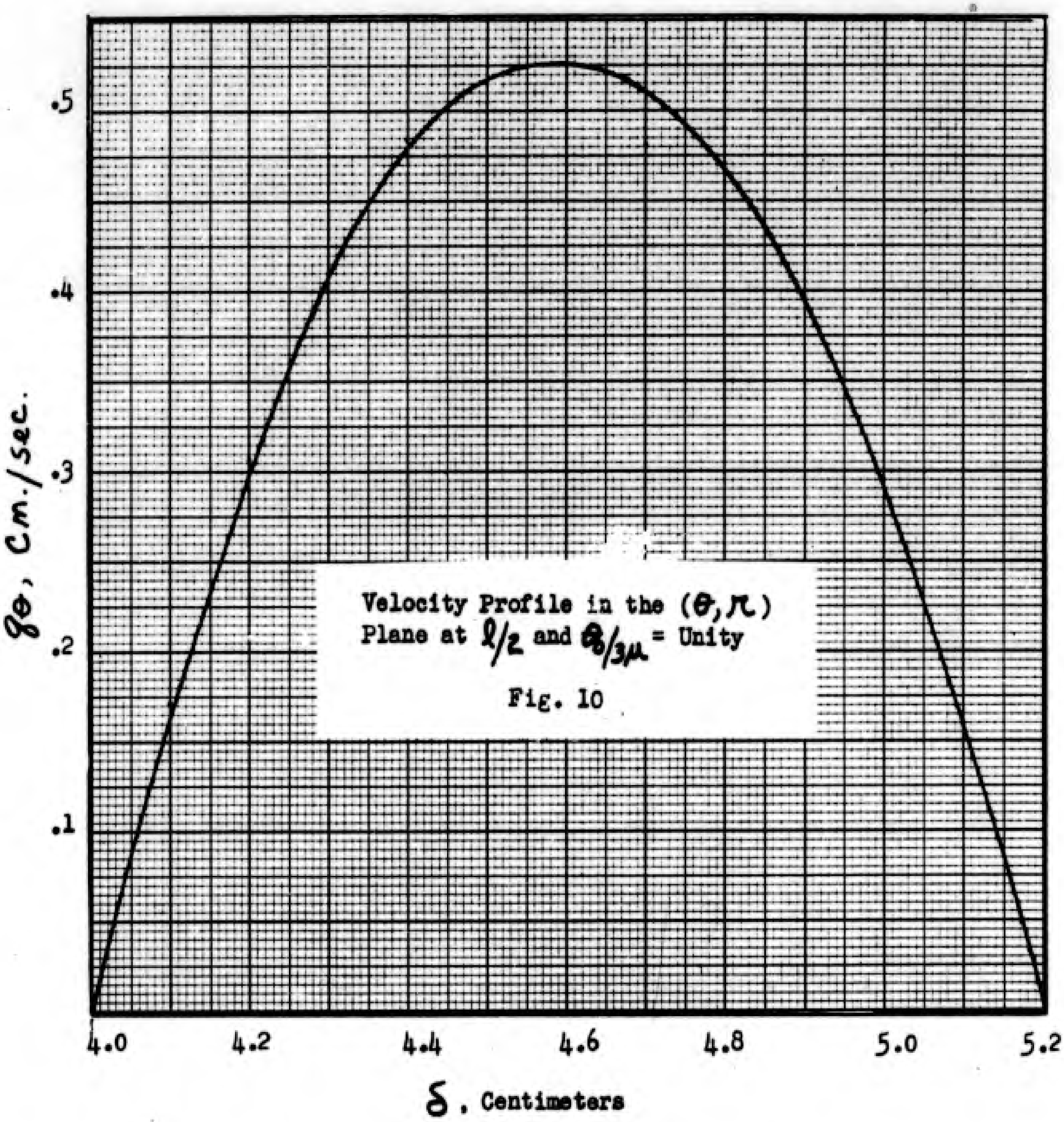

Velocity Profile in the (θ, r) Plane at $l/2$ and $\theta/3\mu$ = Unity

Fig. 10

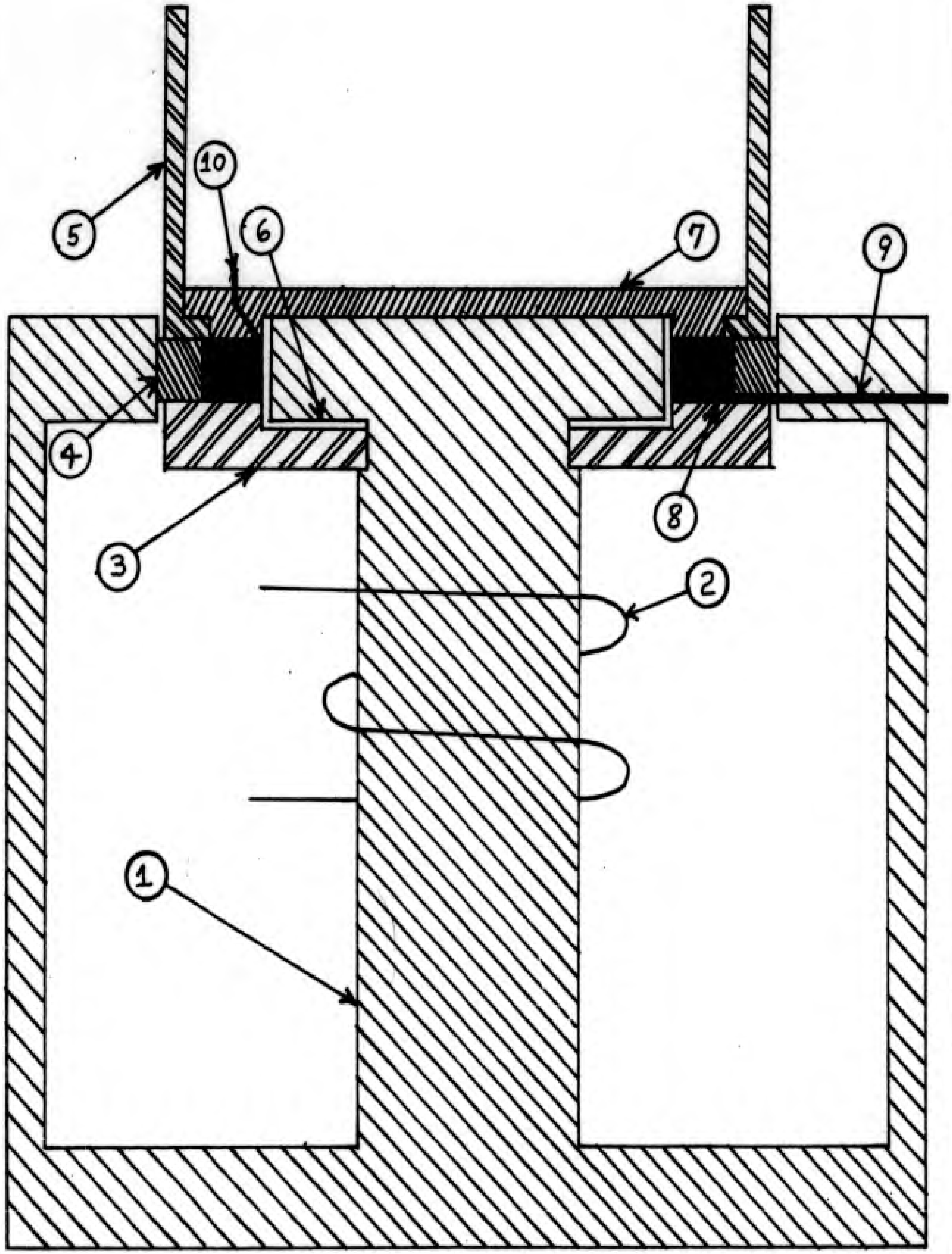

Cross Sectional View of Centrifuge Configuration

Fig. 11

III. Description of Apparatus

Development Model

Figure 11, which faces this page, is a cross-sectional view of the configuration used to produce crossed fields in an annulus, and to obtain data reported in this paper. The sketch shown is not to scale, but it does represent the final design of the centrifuge which is completely circular when viewed from the top. A list of the various components and a brief description of each follows:

1. An electro-magnet is formed by placing a central core in a hollow cylinder which is closed at one end. The magnetic flux path is completed radially through the pole faces formed by extensions of the central core and cylinder at the open end.

2. The hollow space between the cylinder and core is filled by 5660 turns of field windings. This electro-magnet was capable of producing 2500 gauss across the annulus at a field current of 1.5 amperes and an input power of 105 watts.

3. A brass conduction base is nickle plated to inhibit amalgamation. This base forms the bottom of the annulus, and allows conduction from the mercury to the inner core.

4. This component is a plastic ring which serves as the outer vertical wall of the annulus, and as a support for part 5. The plastic ring also insulates the mercury from the outer pole face.

5. A conduction cylinder, also nickle-coated brass, has a small ledge (3/32") which allows current to pass through the mercury to the

conduction base. In order to insure uniform current density, 24 leads were placed around the top periphery of the conduction cylinder. When the width of the rotating ring of mercury is equal to or less than the width of the ledge, current distribution is, for all practical cases, vertical.

6. Plastic insulation was used to prevent horizontal conduction from the conduction cylinder to the inner pole face.

7. A clear plastic cover was bolted to the top of the assembly to form the top of the annulus, to hold the conduction cylinder, and to provide visual access to the chamber.

8. The annulus itself has the dimensions of $R_1 = 4.0$ cm, $R_2 = 5.2$ cm, and $\ell = 1$ cm. The chamber was sealed by using a non-hardening gasket material.

9. Mercury was gravity fed into the annulus chamber through a radial line as shown. For starting, the annulus had to be completely full because the mercury had to be in contact with the conduction ledge. After the mercury had reached a sufficient velocity, a rotating ring of any desired width could be formed by gravity feeding mercury out of the same radial line.

10. A vacuum relief line was installed at the inner pole face for obvious reasons.

The whole assembly, which weighed approximately 100 pounds, had an outside diameter of 9 inches and an overall height of 12 inches. Figure 12 on page 25 shows a photograph of the centrifuge with the

Photograph of Centrifuge
Showing Conduction Leads

Fig. 12

conduction leads attached to the conduction cylinder. A large bus bar used as a ground connection was bolted to the bottom of the centrifuge. The appendix contains a detailed drawing of the development model.

Power Supply

Three 24-volt storage batteries were placed in series to provide a variable field current through a controlling rheostat which was set for low current during switching on and off in order to protect field winding insulation. Separate field excitation was used because of the low voltages and high currents encountered in the armature circuit.

A lack of a suitable power source for the armature circuit restricted the range of experimental data. The source consisted of a 110-volt, 3-phase input to a variac which was used to control a selenium rectifier rated at 200 amps and 24 volts. In order to obtain data, the rectifier was overloaded for short periods to produce currents up to 320 amperes at 1.2 volts. Under these conditions the power was supplied very inefficiently because of the large impedance mismatch between the source and the centrifuge. Only 94 of the supplied 384 watts were measured across the terminals of the centrifuge - the rest being dissipated in the internal impedance and bus bars of the rectifier, and in the power cables. The input power to the mercury armature was estimated to be approximately 5 watts (method of estimation is shown in the appendix). Figure 13 on page 27 shows the experimental setup.

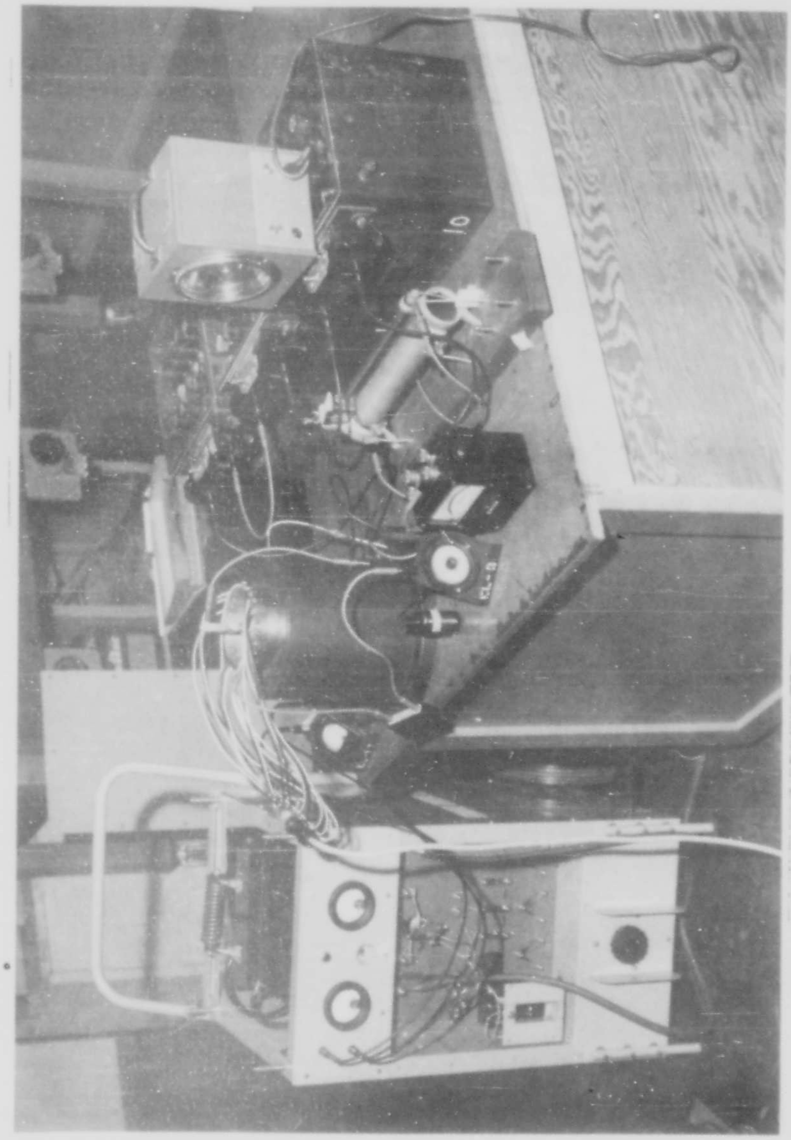

Experimental Setup

Fig. 13

IV. Test Results

Magnetic Flux Density

All of the magnetic field measurements were taken with a GRH Hall Test flux measuring device. Flux density could be read directly in gauss by placing the precision probe furnished with the equipment into the air gap of the empty annulus.

Figure 14 on page 29 shows the variation of flux density with field current at both R_1 and R_2. The slight scattering of points was probably caused by the fact that readings were dependent upon keeping the probe exactly vertical. It is seen from the figure that the flux density is approximately 1000 gauss higher at R_1 than at R_2. This distribution undoubtedly helps to compensate for the poor current distribution during starting and did not appear to cause any noticeable effects once a mercury ring had been formed.

From Fig. 15 on page 30, it is seen that the flux density varies around the periphery of the annulus. The distribution shown suggests that the center core might be slightly off center. This was verified by taking measurements which showed a maximum diametrically opposite difference of approximately 1/32" between pole faces. Further non-linearities could have been introduced by the poor quality of iron used and the drain and fill line which was drilled radially through the outer pole face. The maximum difference between any two points is 105 gauss, and a trapezoidal rule approximation of average flux is 1745 gauss. Percentage deviation from the average flux is 6 percent.

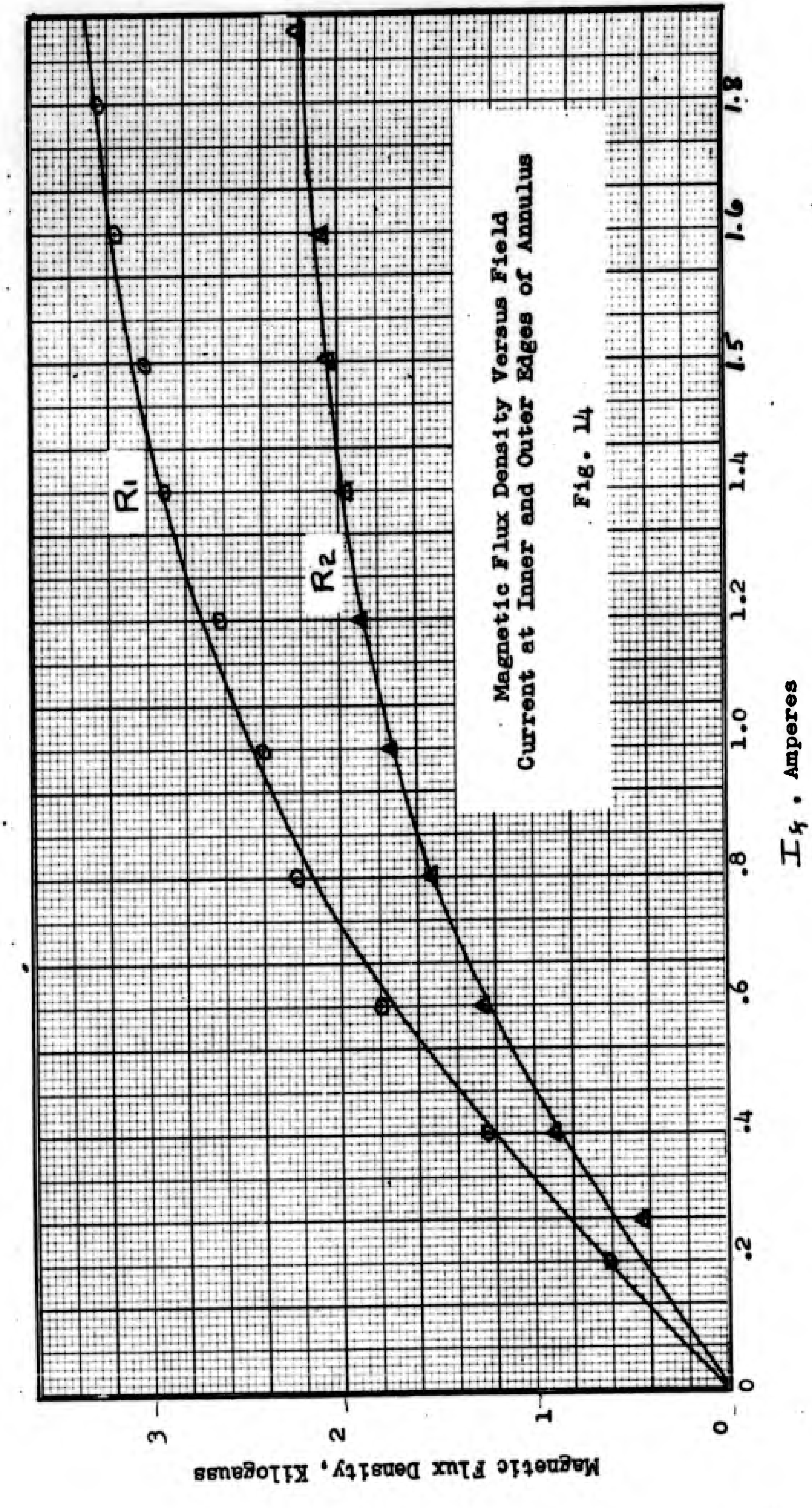

Magnetic Flux Density Versus Field Current at Inner and Outer Edges of Annulus

Fig. 14

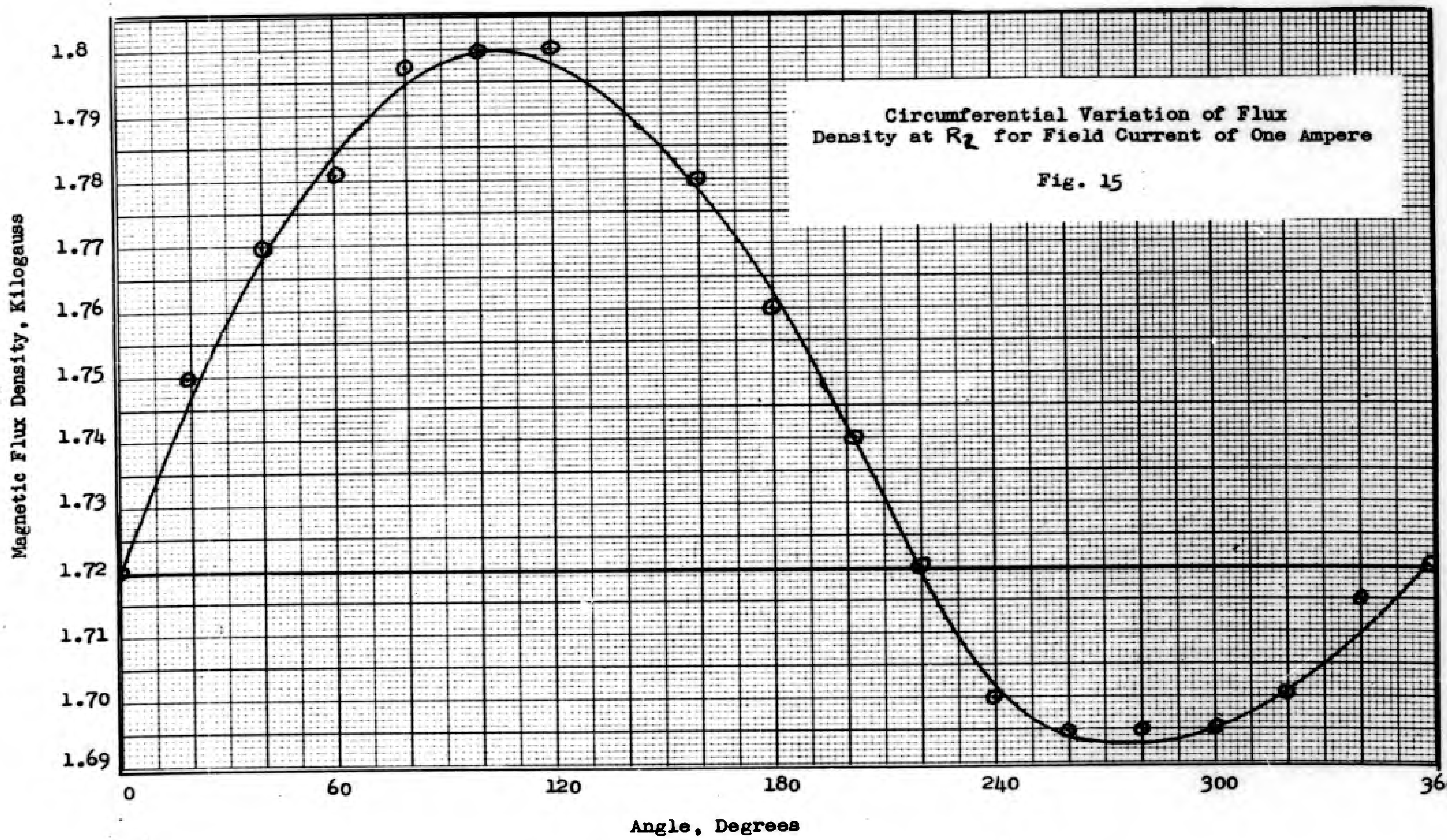

Circumferential Variation of Flux Density at R_2 for Field Current of One Ampere

Fig. 15

Mercury Velocity

Unexpected difficulties were encountered during all attempts to measure mercury velocity. Four different methods of attack were used in an effort to solve this problem, and an outline of each method follows.

First, it was felt that velocity could be calculated by measuring the induced voltage across the armature. Knowing the induced voltage and the applied field, equation (16) or

$$V_i = B l g_\theta \qquad (16)$$

could be solved for g_θ. This was not the case, however, because no measurable back electromotive force was ever detected. It is believed that V_i was too small compared to ohmic drops to be measured. In order to solve for g_θ using this approach, V_i would have to be distinguished from the voltage drop across the rotating ring of mercury. In addition, it is believed that the varying velocities within the fluid would cause internal induced voltages which would in turn create transverse and vertical currents. Resistance across the terminals of the centrifuge was calculated by turning off the applied field and measuring the terminal voltage and amperage. The terminal resistance was found to be only 9.18×10^{-4} ohms which is still much larger than the ohmic drop across the annulus. During rotation with a full annulus, no detectable change in terminal voltage was observed.

The second attempt to calculate velocity involved the use of equation (26) which was solved for pressure differences and written as

$$P_2 - P_1 = \int_1^2 \rho\, q_\theta^2(r)\, dr/r \tag{48}$$

If a thin ring of mercury is considered, the velocity distribution can be assumed to be linear. The velocity function squared over r can then be integrated over R_1 to R_2 to obtain the pressure difference between the inner and outer surfaces of the mercury. In an attempt to measure this pressure difference, a radial pressure tap was installed in the centrifuge. This pressure line was perpendicular to mercury flow, however, and a venturi tube effect created a vacuum in the line rather than indicating correct pressures.

As a third approach, a pitot tube constructed of hypodermic tubing was inserted into the rotating mercury. This method also proved to be impractical because of the turbulence created by the tube and because of the difficulty of trying to calibrate such a device.

Finally, it was decided that a strobo tachometer had to be used for RPM measurements. Since it is impossible to strobe the free surface of a moving liquid, numerous objects in a solid, semi-solid, and liquid state were placed in the centrifuge in an attempt to form a pattern that could be "stopped" by the strobe. All of these objects were centrifuged and carried along by the inner surface of the rotating mercury, but in most cases no readable pattern was formed. The highest measurable velocity was obtained by placing a 1/16" diameter plastic sphere in the chamber. An RPM reading of 2400 was measured using this sphere, but the motion was highly erratic. This erratic motion, which was characteristic of all single objects placed in the chamber, was caused by tumbling between the mercury inner surface, the inner pole face, and the top and bottom of the chamber.

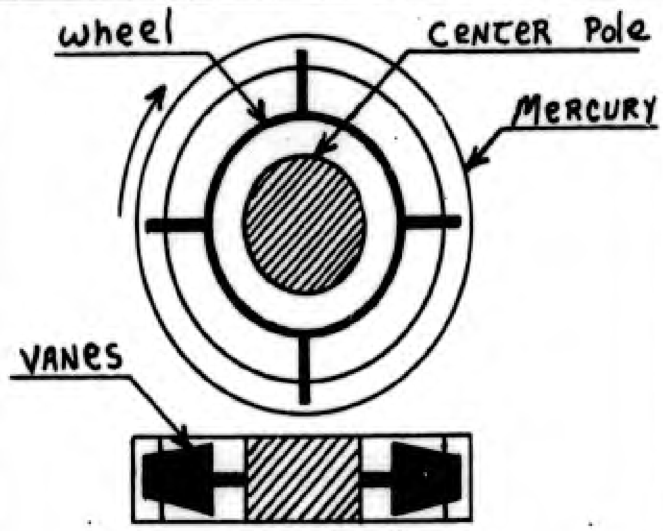

Fig. 16

Paddle Wheel Device Used to Measure RPM

Next, a "friction clutch" was constructed by forming a ring of emery paper stiffened by a cardboard back. This device rode smoothly on the inner surface of the mercury, but a maximum RPM of only 1100 was obtainable. The most successful of the various devices used appears in Fig. 16. A paddle wheel was constructed by cementing plastic vanes on a thin plastic ring. These vanes extended outward into the mercury. Although the paddle wheel gave smooth results, it was still an inefficient device which only gave a rough indication of mercury velocity. Frictional losses, poor dynamic stability, and induced turbulence all served to reduce efficiency. All of the velocity measurements recorded in this report were obtained by strobing the paddle wheel device shown in Fig. 16 with an Electronics Measurements Co. 351-A strobo tachometer. Actual mercury velocity is considered to be much higher than velocities recorded, but the general speed characteristics as shown should be valid.

Figure 17 on page 35 shows paddle wheel RPM versus armature current at two values of mercury ring widths. The two lower points on the plots indicate the RPM at which the mercury rings, no longer supported, collapse, and break contact. Arcing in the chamber occurred at these points because of the intermittent contact between the mercury and the conduction ledge. From Fig. 17, it is seen that both curves are tending to level out at higher RPMs. This is probably due to the increased frictional drag on the paddle wheel rather than the mercury itself. The curve plotted for the smaller ring width indicates a larger body force which is predicted by the theory.

The curves shown in Fig. 18 on page 36 have a greater degree of curvature. This is obviously caused by the fact that the electromagnet is rapidly saturating at the values of field current used. These curves have the same general shape as the flux density versus field current graphs in Fig. 14. Readings could not be taken below 600 RPM with the strobe used, but the rings broke contact at a field current of .25 amperes. The rotating rings at RPMs below 700 were characterized by a swirling, unstable flow. At lower speeds, the inner surface of the mercury was parabolic between the top and bottom of the annulus.

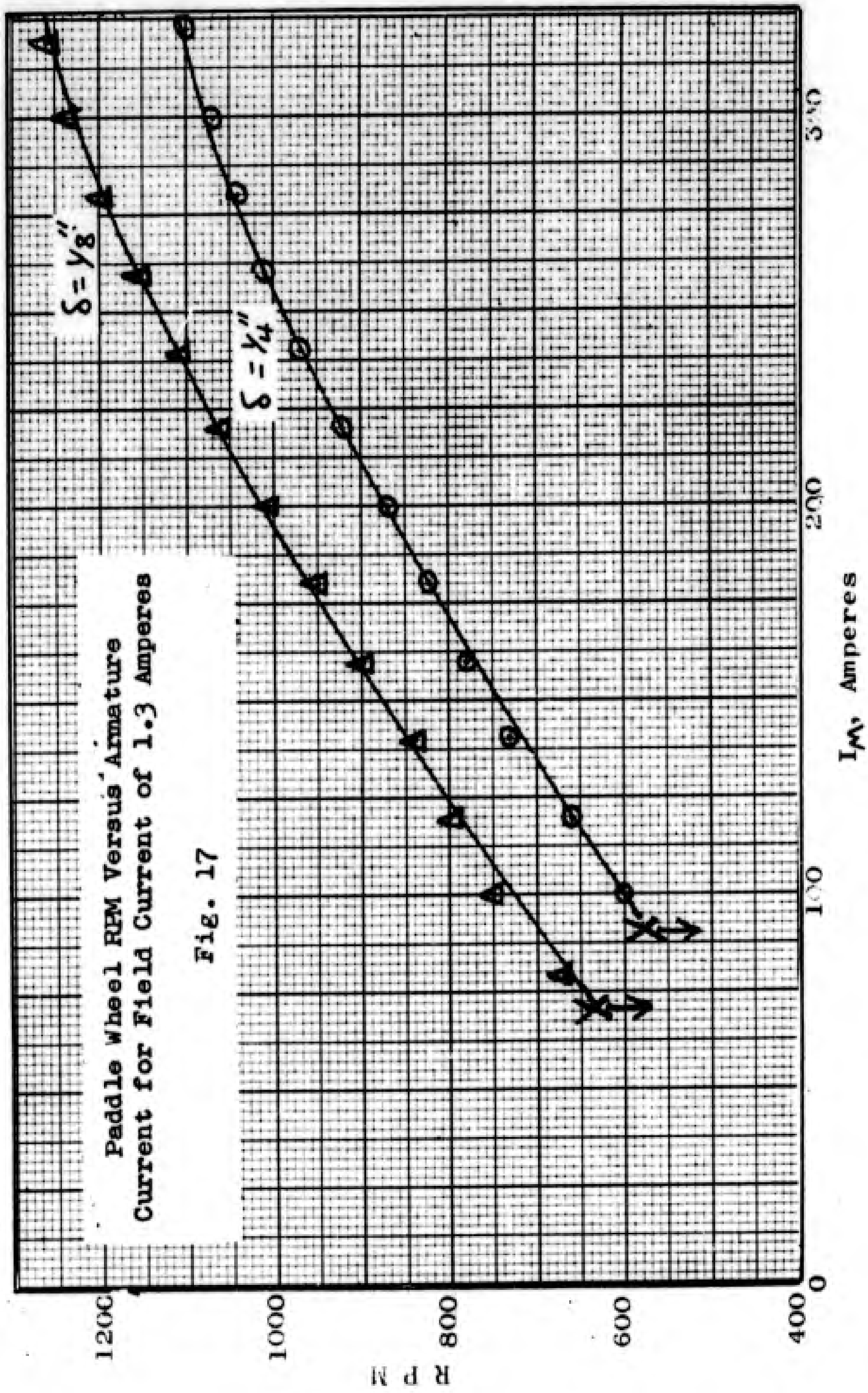

Paddle Wheel RPM Versus Armature Current for Field Current of 1.3 Amperes
Fig. 17
δ = 1/8"
δ = 1/4"
R P M
1200
1000
800
600
400
0
100
200
300
I_M, Amperes

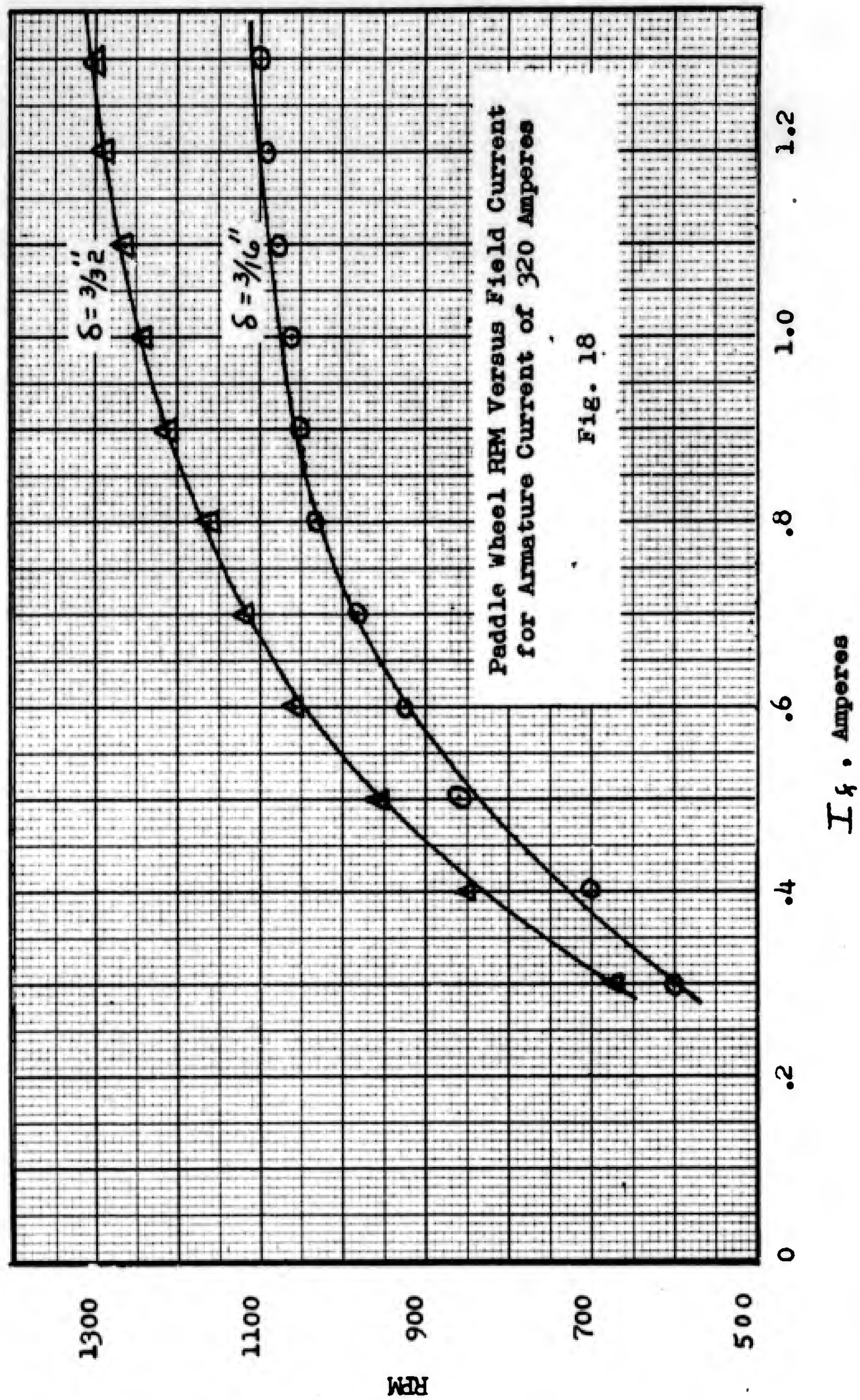

Paddle Wheel RPM Versus Field Current for Armature Current of 320 Amperes

Fig. 18

The most revealing characteristic of the rotating mercury is shown on page 38 in Fig. 19 which is a plot of RPM versus ring width. If this figure is compared with Fig. 4, it is seen that RPM increased as θ_0 increased. As the ring width decreased below 1/16", mercury flow became abrubtly unstable. At this point RPM readings suddenly jumped to 1700 which seems to indicate that the vanes of the paddle wheel were more efficient in turbulent, unstable flow. The two points plotted off the faired curve were measured during this unstable flow. Mercury flow became highly erratic at 1900 RPM, and, after heavy arcing, contact was broken. If the actual velocity of the mercury inner surface could have been measured, ring width could have been used to calculate body force from which an empirical relationship between V_0 and θ_0 could have been found. Ring width was measured by placing a scale on top of the plastic cover. This procedure had its limitations, however, because the rings formed usually had a slight variation in width with circumference.

Stability

The development model ran smoothly without vibration at ring widths as thin as 1/16" when the centrifuge was properly leveled. At ring widths less than 1/16", flow became conditionally unstable. Instability was characterized by an abrupt "wobbling" of the rotating ring of mercury which then appeared to be moving in traveling waves around the annulus. This instability, if allowed to continue at even thinner ring widths, became violent enough to vibrate the centrifuge

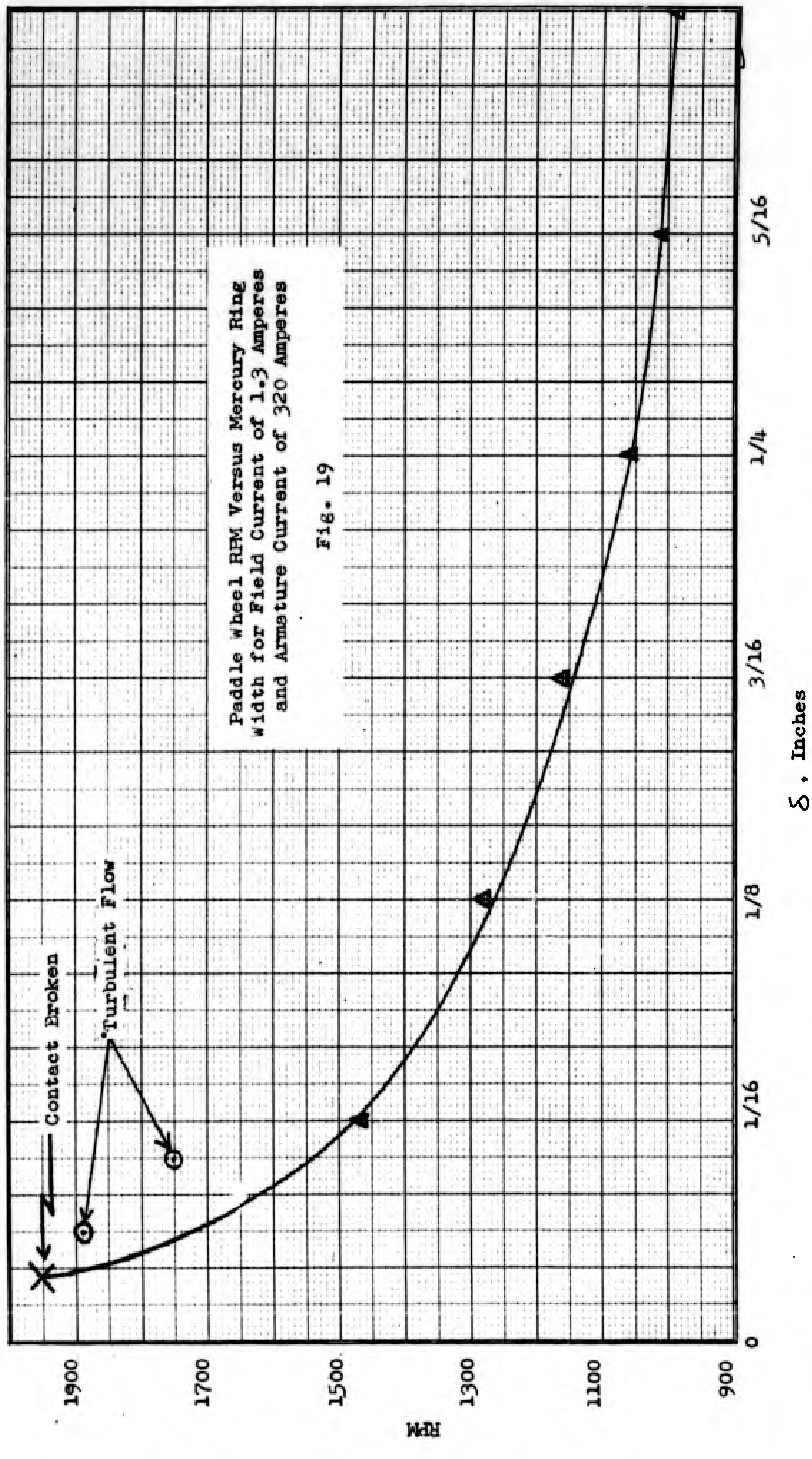

Paddle wheel RPM Versus Mercury Ring Width for Field Current of 1.3 Amperes and Armature Current of 320 Amperes

Fig. 19

assembly. In one instance, .5 cubic centimeters of mercury spread into a thin rotating film, caused the centrifuge to vibrate along the laboratory table. Rings rotating in this manner served as intermittent conductors between the conduction ledge and base, and caused heavy arcing in the annulus chamber.

It is believed that the instability described above is caused by poor dynamic balance due to varying width around the rings circumference, and by a separation of the thin film of mercury by wall shearing forces. Both dynamic unbalance and varying width would, in turn, produce uneven body forces. Once instability occurred, it was impossible to dampen the oscillations until the annulus was almost completely refilled with mercury. The strength of the applied magnetic field had no noticeable effect upon stability. This seems to emphasize the mechanical rather than magneto-hydrodynamic nature of the instability.

By tilting the centrifuge only slightly from the vertical, instability could be induced at ring widths of approximately 1/4". The type of flow produced in this manner again appeared to be in traveling waves, but less violent and without arcing. No noticeable effects were noted when operating the centrifuge with 6 of the conduction leads detached in a random pattern.

<u>Qualitative Observations</u>

The nature of the rotating rings formed, depended upon the condition of the mercury, the presence of foreign objects in the chamber, and the rate of formation. With clean mercury, very thin, uniform rings with smooth, near vertical inner surfaces could be formed. The slow amalgamation of the nickle-plated surfaces, and oxidation caused by arcing, produced slag in the mercury. This slag, if not removed, tended to disturb the pattern of flow and to create turbulence. Foreign objects extending into the mercury created disturbances which were reflected around the circumference of the annulus. These reflected disturbances produced maximum and minimum ring widths in the form of a standing wave. One characteristic standing wave always appeared with two maximums and two minimums. A minimum of this standing wave was located near the radial drain and fill line which was evidently causing the disturbance. The characteristic wave could be formed by rapidly draining mercury from the annulus.

Mercury flow during normal operation was undoubtedly turbulent to some degree, but it was difficult to determine whether mixing was taking place by viewing the inner surface. Capillary waves, which were described in a recent paper on free surface mercury studies, covered the inner mercury surface with a fine pattern of intersecting lines. Irregularities which might appear with the onset of turbulence would be hard to see in the presence of capillary patterns (Ref. 8:761).

Even after arcing, mercury temperatures were only slightly higher than room temperatures at armature currents up to 320 amperes. Conductive heating from the electro-magnetic core became apparent, however, after extended periods of operation.

V. Conclusions and Recommendations

The general theory of magneto-hydrodynamics was applied to the case of mercury being used as a direct-current motor armature. A supposition was then made that this armature could be used as a centrifuging device. From the theory, a prototype magneto-hydrodynamic centrifuge was designed and tested in an effort to determine its feasibility. Available power sources restricted experimentation to low power inputs; however, a number of conclusions and recommendations can be drawn from the data obtained and from qualitative observation.

Conclusions

In general, test results show that the basic operational principle of the centrifuge is sound and feasible. Rotating rings of mercury were formed which drove a paddle wheel at a measurable 2000 RPM at an estimated mercury input power of 5 watts. Because of paddle wheel inefficiencies, actual mercury velocity is considered to be higher than measured RPM. Considering the fact that electro-magnetic pumps have been designed to handle currents as high as 20,000 amperes, the performance of the development prototype gives only a hint of the potential capabilities of a magneto-hydrodynamic centrifuge. In addition, the following more specific conclusions are made:

1. The determination of actual mercury velocity by the instrumentation techniques outlined in this report do not appear to be feasible.

2. A flux homogeneity deviation of 6 percent does not cause any noticeable effect on stability at estimated mercury velocities up to 4000 RPM.

3. Requirements for uniform current distribution are not critical at the rotational speeds achieved.

4. Mercury Joule heating is negligible at armature currents up to 320 amperes.

5. Normal direct-current power supplies are not suitable because of the large impedance mismatch between the source and the centrifuge.

6. Stability is dependent upon vertical alignment of the centrifuge, upon mercury ring width, and upon induced turbulence.

Recommendations

Further investigation of the centrifuge is needed because available sources restricted experimentation to low power inputs. The following recommendations are made for future study:

1. An effort should be made to design a more suitable power supply. The most promising source seems to be a Homopolar Generator described in the literature as being capable of supplying currents in excess of 20,000 amperes at .5 volts with efficiencies of 50 to 60 percent (Ref. 9-16).

2. Thought should be given to optimizing the annulus dimensions with respect to current and flux distribution, conductivity, wall shearing forces, and electrical contacts.

3. A more suitable material should be substituted for the nickle-plated surfaces which began to amalgamate after extended periods of contact with mercury.

4. The centrifuge should be mounted on an adjustable platform because of stability dependence upon vertical alignment.

5. Continued research for a suitable method of measuring mercury velocity is needed.

Finally, it is hoped that the conclusions and recommendations, as outlined above, prove to be an aid in the future investigation of this study which remains an interesting and challenging one.

Bibliography

1. Resler, E. L., Jr., and W. R. Soars. "The Prospects for Magnetohydrodynamics." Journal of the Aeronautical Sciences, 25:236-237 (April 1958).

2. Binder, R. C. Advanced Fluid Mechanics. New York: Prentice-Hall, Inc., 1958.

3. Blake, L. R. "Conduction and Induction Pumps for Liquid Metals." Proceedings of the Institute of Electrical Engineers, 104: Pt. A, 59-50 (1957).

4. Monopoli, V. "The Development of a Magnetohydrodynamic Gyroscope." Proceedings of the National Electronics Conference, 16:369-375 (1960).

5. Hartmann, J., and F. Lazarus. "Experimental Investigation of Mercury in a Homogenous Magnetic Field." Det Kgl. Danshe Vidensbabernes. Selskab Mat. - Fys, Medd., 15, No. 6; 7 (1937).

6. Murgatroyd, W. "Experiments on Magneto-Hydrodynamical Channel Flow." Philosophical Magazine, 44:1348-1350 (1953).

7. Lydoudis, P. S. "Transition From Laminar to Turbulent Flow in Magneto-Fluid Mechanic Channels." Reviews of Modern Physics, 32:796-798 (October 1960).

8. Alpher, R. A., et al. "Some Studies of Free-Surface Mercury Magnetohydrodynamics." Review of Modern Physics, 32:758-766 (October 1960).

9. Barnes, A. H. "Direct Current Electromagnetic Pumps." Nucleonics, 45:16-18 (January 1953).

10. Wylie, C. R., Jr. Advanced Engineering Mathematics, (Second Edition). New York: McGraw-Hill Book Company, Inc., 1960.

Appendix

Solution of Equation (27)

Given:

$$0 = \theta_0 + \mu\left(d^2 g_\theta/dr^2 + \frac{1}{r}\, dg_\theta/dr - g_\theta/r^2\right) \tag{27}$$

Multiplying through by r^2 and dividing through by μ yields

$$0 = \frac{\theta_0}{\mu} r^2 + r^2 d^2 g_\theta/dr^2 + r\, dg_\theta/dr - g_\theta \tag{A-1}$$

Equation (A-1) is, except for the forcing function $\frac{\theta_0}{\mu} r^2$, Cauchy's equation in which the coefficient of each derivative is proportional to the corresponding power of the independent variable (Ref: 10:111). Under the transformation

$$r = e^z \quad \text{OR} \quad z = \ln r \tag{A-2}$$

we have

$$dg_\theta/dr = dg_\theta/dz \cdot dz/dr = \frac{1}{r}\, dg_\theta/dz \tag{A-3}$$

and

$$d^2 g_\theta/dr^2 = \frac{d}{dr}\left(\frac{1}{r}\, dg_\theta/dz\right) = -\frac{1}{r^2}\, dg_\theta/dz + \frac{1}{r}\, d^2 g_\theta/dz^2\, dz/dr$$

$$= -\frac{1}{r^2}\, dg_\theta/dz + \frac{1}{r^2}\, d^2 g_\theta/dz^2 \tag{A-4}$$

Substituting (A-3), (A-4), and $r = e^z$ into (A-1) yields

$$0 = \frac{\theta_0}{\mu}(e^z)^2 + (e^z)^2\left[-\frac{1}{(e^z)^2}\, dg_\theta/dz + \frac{1}{(e^z)^2}\, d^2 g_\theta/dz^2\right] + e^z\left(\frac{1}{e^z}\, dg_\theta/dz\right) - g_\theta$$

Simplifying and collecting terms we have

$$d^2 g_\theta / dz^2 - g_\theta = -\frac{\theta_0}{\mu} e^{2z} \tag{A-5}$$

The characteristic solution to (A-5) is

$$g_\theta = A_1 e^{-z} + A_2 e^{z}$$

and a particular solution to (A-5) is

$$-\frac{\theta_0}{3\mu} e^{2z}$$

Therefore the complete solution is

$$g_\theta = A_1 e^{-z} + A_2 e^{z} - \frac{\theta_0}{3\mu} e^{2z} \tag{A-6}$$

Finally, replacing z by $\ln r$ in (A-6) yields

$$\begin{aligned} g_\theta(r) &= A_1 e^{-\ln r} + A_2 e^{\ln r} - \theta_0/3\mu \, e^{2\ln r} \\ &= A_1 r^{-1} + A_2 r - \frac{\theta_0}{3\mu} r^2 \end{aligned} \tag{28}$$

Sample Calculations

Electric Body Force, θ_o . Given that I_m = 30 abamperes, B_r = 1600 gauss, R_1 = 5.0 cm., R_2 = 5.2 cm., θ_o in dynes/cm.^{3} is found as follows:

$$\theta_o = \vec{j}_z \times \vec{B}_r = \frac{I_m B}{\pi(R_2^2 - R_1^2)} = \frac{(30)(1600)}{\pi(5.2^2 - 5.0^2)}$$

= 7500 dynes/cm.^{3}.

θ_o in lbs/ft^3 is found by

$$\theta_o,\ \text{lbs/ft}^3 = 7.5 \times 10^3 \ \frac{\text{dynes}}{\text{cm}^3} \times 2.248 \times 10^{-6} \ \frac{\text{lbs}}{\text{dynes}} \times 28.3 \times 10^3 \ \frac{\text{cm}^3}{\text{ft}^3}$$

= 478 lbs/ft^3.

The above calculation assumes that armature current and magnetic flux are mutually perpendicular. Verification of the cgs units used in the above calculation for force is shown as

$$BI_m = \text{Gauss} \ \frac{\text{Abamperes}}{\text{cm}^2} = \frac{\text{Maxwell}}{\text{cm}^2} \ \frac{\text{Abcoulomb}}{\text{sec-cm}^2}$$

$$= \frac{\text{Abvolt-sec}}{\text{cm}^2} \ \frac{\text{Abcoulomb}}{\text{sec-cm}^2} = \frac{(\text{dyne-sec})}{\text{abcoulomb cm}} \ \frac{(\text{Abcoulomb})}{\text{sec-cm}^2}$$

$$= \frac{\text{dyne}}{\text{cm}^3}$$

Reynold's Number. Calculation of Re for $g_{\theta AV}$ = 50 ft/sec, ν = 1.14 x 10^{-7} mtr^2/sec, and characteristic length L = δ = .2 x 10^{-2} mtrs is found by

$$Re = g_{\theta AV}\,\delta/\nu = \frac{50 \text{ ft/sec} \ \frac{.305 \text{ mtr}}{\text{ft}} \times .2 \times 10^{-2} \text{ mtrs}}{1.14 \times 10^{-7} \text{ mtr}^2/\text{sec}} =$$

2.67 x 10^5 (Dimensionless)

Hartmann Number. Calculation of M for B = .16 Webers/mtr^2, ρ = 1.35 x 10^4 kg/mtr^3, L = δ = .2 x 10^{-2} mtrs, ν = 1.14 x 10^{-7} mtr^2/sec, and 1/ σ = 94.1 x 10^{-8} ohm-mtrs is found by

$$M = B\delta\left(\sigma/\rho\nu\right)^{\frac{1}{2}} = \frac{(.16)(.2) \times 10^{-2}}{\left[(94.1 \times 10^{-8})\,(1.35 \times 10^{4})\,(1.14 \times 10^{-7})\right]^{\frac{1}{2}}}$$

$$= \frac{32 \times 10^{-5}}{3.82 \times 10^{-5}} = 8.40 \text{ (Dimensionless)}$$

Estimation of Transition from Laminar to Turbulent Flow. Using the same constants as in the Re and M calculations above, transition is estimated by

$$\frac{Re}{M} \cong 236, \quad g_\theta\,\text{(Transition)} = \frac{236\,M\,\nu}{\delta}$$

$$= \frac{(236)\,(8.40)(1.14) \times 10^{-7}}{2 \times 10^{-3}} = 11.3 \times 10^{-2} \text{ mtrs/sec}$$

$$= 11.3 \text{ cm/sec}$$

Estimation of Mercury Input Power. Given that armature RPM = 4000, I_m = 300 amperes, B = .16 Weber/mtr^2, ℓ = 1 x 10^{-2} mtrs, and δ = .2 x 10^{-2} mtrs, input power is estimated as follows:

$$g_\theta, \text{ ft/sec} = (2\pi r)\frac{(\text{RPM})}{60} = 2\pi(1/6)(66.7) = 69 \text{ ft/sec}$$

Assuming that the velocity distribution is linear from the mercury surface to the zero vertical boundary at thin ring widths, and assuming that the velocity is parabolic between the top and bottom of the annulus, an average velocity is given by

$$g_{\theta_{AV}} = g_\theta \times 1/2 \times 2/3 = 23 \text{ ft/sec}$$

where the factor 1/2 is a correction for the linear distribution and the factor 2/3 is a correction for the parabolic distribution. Induced voltage is then found by

$$V_i = B \ell g_{\theta AV} = \frac{\text{Weber}}{\text{Mtr}^2} \text{Mtr} \frac{\text{Mtr}}{\text{Sec}} = \frac{\text{Weber}}{\text{Sec}} = \text{Volt}$$

Converting $g_{\theta AV}$ to mtr/sec, V_i becomes

$$V_i = (.16)\ 10^{-2}\ (23)\ (.305) = 112 \times 10^{-4}$$

$$= .0112 \text{ volts}$$

Power input to the mercury neglecting

$I_M^2 R_M$ loss is then

$$P_M = V_i I_M = 3 \times 10^2 \times 1.12 \times 10^{-2} = 3.36 \text{ watts}$$

A check on the order of magnitude of P_M can be shown by

$$P_M = F g_{\theta AV} = (.12 \text{ lbs})\ 23 \frac{\text{ft}}{\text{sec}} \left(\frac{746 \text{ watts}}{550 \text{ ft-lb/sec}} \right)$$

$$= 3.74 \text{ watts}$$

where .12 lbs is the force calculated for $I_M = 300$ amperes.

The power lost due to mercury heating is found by

$$P_d = I_M^2 R_M = I_M^2 \ell / \sigma A = I_M^2 \ell / \sigma \pi (R_2^2 - R_1^2)$$

$$= \frac{(9 \times 10^4)\ (94.1 \times 10^{-6})\ (1)}{(2.04)} = 1.32 \text{ watts}$$

The total input power to the mercury is then approximated by

$$P_T = P_M + P_d = 3.36 + 1.32 = 4.68 \text{ watts}$$

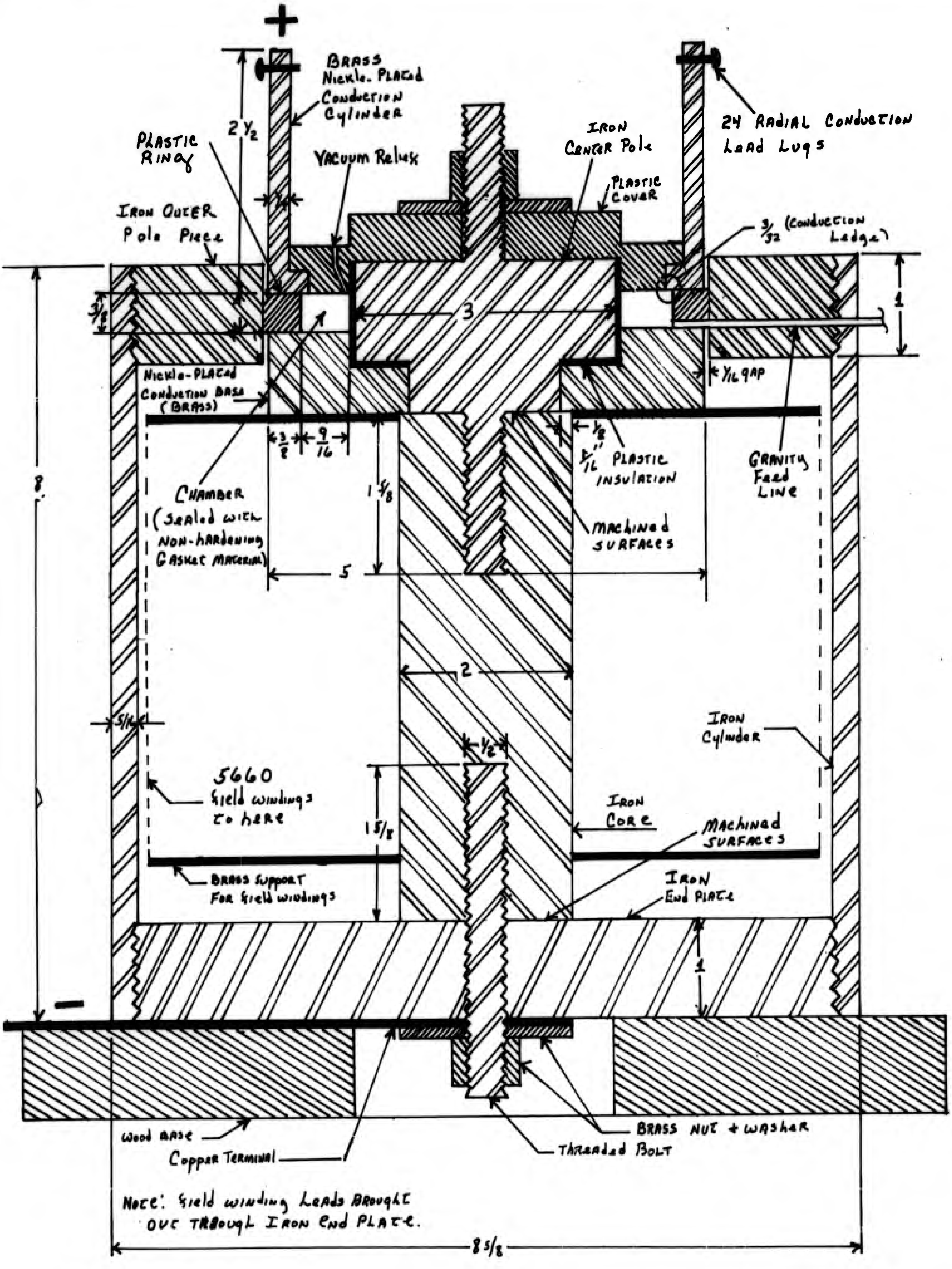

Detailed Drawing of Development Prototype

Fig. 20

Vita

Luin Blunt Ricks was born on [redacted]

After completing his work in [redacted], he enrolled at Northwestern University, Chicago. He served in the US Navy as an enlisted man from 1948 to 1950. Upon his discharge, he enrolled in the US Naval Academy, Annapolis, Maryland, and in June 1954 he was graduated with the degree of Bachelor of Science. After receiving his commission as Lieutenant in the USAF, he entered active duty in June 1954. His military assignment prior to his coming to the Air Force Institute of Technology was as Pilot Flight Examiner in the Military Air Transport Service.

Permanent address: [redacted].

This thesis was typed by Mrs. Joyce M. Andrews.

UNCLASSIFIED